Nonlinear ionic transport through microstructured solid electrolytes: homogenization estimates

2016 Modelling Simul. Mater. Sci. Eng. 24 075008

(http://iopscience.iop.org/0965-0393/24/7/075008)

IOP Publishing Modelling and Simulation in Materials Science and Engineering

Modelling Simul. Mater. Sci. Eng. **24** (2016) 075008 (16pp) doi:10.1088/0965-0393/24/7/075008

Nonlinear ionic transport through microstructured solid electrolytes: homogenization estimates

Ignacio J Curto Sillamoni[1] **and Martín I Idiart**[1,2]

[1] Departamento de Aeronáutica, Facultad de Ingeniería, Universidad Nacional de La Plata, Avda. 1 esq. 47 S/N, La Plata B1900TAG, Argentina
[2] Consejo Nacional de Investigaciones Científicas y Técnicas (CONICET), CCT La Plata, Calle 8 N° 1467, La Plata B1904CMC, Argentina

E-mail: ignacio.curto@ing.unlp.edu.ar and martin.idiart@ing.unlp.edu.ar

Received 4 February 2016, revised 13 August 2016
Accepted for publication 5 September 2016
Published 29 September 2016

Abstract

We consider the transport of multiple ionic species by diffusion and migration through microstructured solid electrolytes in the presence of strong electric fields. The assumed constitutive relations for the constituent phases follow from convex energy and dissipation potentials which guarantee thermodynamic consistency. The effective response is heuristically deduced from a multi-scale convergence analysis of the relevant field equations. The resulting homogenized response involves an effective dissipation potential per species. Each potential is mathematically akin to that of a standard nonlinear heterogeneous conductor. A 'linear-comparison' homogenization technique is then used to generate estimates for these nonlinear potentials in terms of available estimates for corresponding linear conductors. By way of example, use is made of the Maxwell-Garnett and effective-medium linear approximations to generate estimates for two-phase systems with power-law dissipation. Explicit formulas are given for some limiting cases. In the case of threshold-type behavior, the estimates exhibit non-analytical dilute limits and seem to be consistent with fields localized in low energy paths.

Keywords: electrochemistry, composites, nonlinearity, variational methods

(Some figures may appear in colour only in the online journal)

1. Introduction

At room temperature, the transport of ions through many solid electrolytes is believed to occur by a hopping mechanism whereby, under the action of an electric field, ions jump along

coordination sites available throughout the solid. Under moderate electric field intensities this mechanism results in a nonlinear relation between the current density of electric charge and the electric field intensity (e.g. Heuer *et al* (2005)). In the presence of multiple microstructural phases, the macroscopic conductivity is dictated to a first approximation by the local transport properties of each phase and their geometric arrangement.

The problem of correlating the macroscopic and local transport properties in *linear* electrolytes with an arbitrary number of ionic species has been recently addressed by Curto Sillamoni and Idiart (2015). Thermodynamically consistent field equations were first derived following the work of Xiao and Bhattacharya (2008) and then homogenized by means of the notion of multi-scale convergence of Allaire and Briane (1996). The resulting description of the overall response requires the solution of a standard conductivity problem over the representative volume element per ionic species. These conductivity problems are only coupled at the macroscopic level, and so well-known results for linear heterogeneous conductors can be used as is at the microscopic level.

The above approach is generalized here, albeit heuristically, to *nonlinear* systems. Thus, the resulting description of the overall response requires the solution of several decoupled conductivity problems that can be treated by available homogenization techniques for standard nonlinear heterogeneous conductors. In this work we explore the use of a 'linear-comparison' technique proposed in the mathematically analogous context of nonlinear heterogenous dielectrics by Ponte Castañeda (2001). This technique makes use of a linear comparison solid with the same microgeometry as the nonlinear solid but with linearized local responses whose overall response can be determined with linear approximations such as the well-known Maxwell-Garnett or effective-medium approximations. A suitably designed variational principle is then used to select the optimal linearization parameters within a given class of linearization schemes to produce the best possible nonlinear estimates in terms of the available linear estimates. A distinguishing feature of this technique is that the linearization scheme corresponds to a generalized secant approximation to the nonlinear local response which depends not only on the phase averages, or first moments of the fields in the phases, but also on the second moments of the intraphase field fluctuations. Consequently, the technique is particularly apt not only for weakly nonlinear responses but also for strongly nonlinear responses which allow the fields to localize along low energy paths (see, for instance, Idiart *et al* (2009)), as in the context, for instance, of dielectric breakdown. By way of example, the technique is applied to three-dimensional two-phase systems exhibiting power-law behavior, which include strongly nonlinear threshold-type behaviors as a limiting case.

2. Ionic transport in microstructured solid electrolytes

2.1. The solid electrolyte model

We consider the transport of ions through a microstructured electrolyte medium composed of N different homogeneous phases and operating under low-frequency isothermal conditions. The electrolyte occupies a geometric domain $\Omega \subset \mathbb{R}^3$, while each phase r occupies a—possibly disconnected—domain $\Omega^{(r)} \subset \Omega$ ($r = 1,...,N$) such that $\Omega = \cup_{r=1}^{N} \Omega^{(r)}$. The domains $\Omega^{(r)}$ can be described by a set of characteristic functions $\chi^{(r)}(\mathbf{x})$, which take the value 1 if the position vector $\mathbf{x}$ is in $\Omega^{(r)}$ and 0 otherwise. The phases contain A different ionic species with valencies z_α ($\alpha = 1, ..., A$). In the presence of an electric field, these ions move through the electrolyte medium and establish an electric current.

The balance of ions requires that

$$\dot{c}_\alpha + \nabla \cdot \mathbf{j}_\alpha = 0 \quad \text{in } \Omega, \quad \alpha = 1, ..., A, \tag{1}$$

where c_α, $\mathbf{j}_\alpha = c_\alpha \mathbf{v}_\alpha$ and $\mathbf{v}_\alpha$ denote, respectively, the molar concentration, the molar flux and the drift velocity of ions of type α within the electrolyte, and the overdot denotes time derivative. In turn, the electric potential $\phi(\mathbf{x})$ in all space is solution to the Maxwell's equations

$$\nabla \cdot \mathbf{d} = F \sum_{\alpha=1}^{A} z_\alpha c_\alpha, \quad \mathbf{d} = \epsilon_0 \mathbf{e} + \mathbf{p}, \quad \mathbf{e} = -\nabla \phi \quad \text{in } \mathbb{R}^3, \tag{2}$$

where F is Faraday's constant, ϵ_0 is the permittivity of vacuum, $\mathbf{d}(\mathbf{x})$ is the electric displacement, $\mathbf{e}(\mathbf{x})$ is the intensity of the electric field, $\mathbf{p}(\mathbf{x})$ is the electric polarization of the electrolyte medium, and $\phi(\mathbf{x})$ is continuous and such that $\phi \to 0$ as $|\mathbf{x}| \to \infty$. Finally, the electric current density $\mathbf{i}(\mathbf{x})$ flowing within the electrolyte is given in terms of the molar fluxes by

$$\mathbf{i} = F \sum_{\alpha=1}^{A} z_\alpha \mathbf{j}_\alpha + \dot{\mathbf{p}} \quad \text{in } \Omega\,. \tag{3}$$

Equations (1) and (2) must be supplemented by suitable constitutive relations. Following the work of Xiao and Bhattacharya (2008), Curto Sillamoni and Idiart (2015) derived the following set of thermodynamically consistent relations:

$$\mathbf{e} = \frac{\partial W}{\partial \mathbf{p}}, \quad \mu_\alpha = \frac{\partial W}{\partial c_\alpha} + F z_\alpha \phi, \quad \mathbf{j}_\alpha = -c_\alpha \frac{\partial U}{\partial (\nabla \mu_\alpha)}. \tag{4}$$

In these expressions, the μ_α are continuous fields representing the electrochemical potentials associated with each species α, and the functions W and U are the free energy density and dissipation potential of the solid electrolyte, respectively. These functions can be written as

$$W(\mathbf{x}, \mathbf{p}, c_1, ..., c_A) = \sum_{r=1}^{N} \chi^{(r)}(\mathbf{x})\; W^{(r)}(\mathbf{p}, c_1, ..., c_A), \tag{5}$$

$$U(\mathbf{x}, \nabla \mu_1, ..., \nabla \mu_A) = \sum_{r=1}^{N} \chi^{(r)}(\mathbf{x})\; U^{(r)}(\nabla \mu_1, ..., \nabla \mu_A), \tag{6}$$

where the $W^{(r)}$and $U^{(r)}$ denote the energy densities and dissipation potentials associated with each phase r. The functions $W^{(r)}$ and $U^{(r)}$ are assumed to be convex. In addition, the functions $U^{(r)}$ are assumed to be positive and to take the value 0 at $\nabla \mu_\alpha = \mathbf{0}$. These properties guarantee positivity of dissipation as required by the laws of thermodynamics.

In this work we assume the more specific forms

$$W^{(r)}(\mathbf{p}, c_1, ..., c_A) = W_p^{(r)}(\mathbf{p}) + RT \sum_{\alpha=1}^{A} c_\alpha \left(\ln \frac{c_\alpha}{c_{0\alpha}^{(r)}} - 1 \right), \tag{7}$$

$$U^{(r)}(\nabla \mu_1, ..., \nabla \mu_A) = \sum_{\alpha=1}^{A} U_\alpha^{(r)}(\nabla \mu_\alpha). \tag{8}$$

Here, $W_p^{(r)}$ is the internal energy stored in phase r by electric polarizability, RT is the universal gas constant times the absolute temperature, $c_{0\alpha}^{(r)}$ is a reference molar concentration

characteristic of phase r, and $U^{(r)}$ is a dissipation potential associated with the ionic mobility through phase r. Introducing these functions in (4) we obtain the following constitutive relations consistent with thermodynamics:

$$\mathbf{e} = \frac{\partial W_p^{(r)}}{\partial \mathbf{p}}(\mathbf{p}), \quad \mu_\alpha = RT \ln \frac{c_\alpha}{c_{0\alpha}^{(r)}} + F z_\alpha \phi, \quad \mathbf{j}_\alpha = -c_\alpha \frac{\partial U_\alpha^{(r)}}{\partial \nabla \mu_\alpha}(\nabla \mu_\alpha). \tag{9}$$

These constitutive relations are suitable for solid electrolytes containing dilute solutions of ions whose contribution to the free energy is due entirely to the entropy of mixing (see, for instance, Hong *et al* (2010)). Any dissipation due to electric polarizability is not considered. Note that when the reference concentrations $c_0^{(r)}$ differ between phases, the molar concentrations c_α are discontinuous across material interfaces. In fact, the ratio $c_{0\alpha}^{(r)}/c_{0\alpha}^{(s)}$ fixes the ratio of molar concentrations of ionic species α in phases r and s under equilibrium conditions. The focus here is on electrolyte systems where the dissipation potentials $U_\alpha^{(r)}$ are non-quadratic and the length scales of the microstructural morphologies are much smaller than the characteristic size of the specimen and the scale of variation of the boundary conditions. The field equations (1) and (2) thus constitute a system of nonlinear differential equations with highly oscillating coefficients. An approximate homogenization procedure to address this problem is considered next.

2.2. The effective response

Homogenization procedures rely on the so-called separation of length scales approximation whereby the characteristic length scale of the microstructural morphologies is taken to be infinitely smaller than the characteristic length scale of the specimen. These procedures yield a set of macroscopic field equations defined over the specimen domain and involving an effective response which requires the solution of a set of microscopic equations defined over a representative volume element of the microstructured solid and involving the local response. The effective response is formally obtained by evaluating the transport of ions through a sequence of material systems with fixed Ω and infinitely decreasing microstructural length scales. Curto Sillamoni and Idiart (2015) have recently evaluated such a limit by making use of the multi-scale convergence approach of Allaire and Briane (1996). Even though their analysis was restricted to quadratic polarization energies and dissipation potentials, we assume here that the structure of the resulting multi-scale system of field equations is preserved for general convex energies and dissipation potentials. We restrict the analysis to steady-state conditions. Thus, the macroscopic field equations are taken to be

$$\nabla \cdot \bar{\mathbf{j}}_\alpha = 0, \quad \nabla \cdot \bar{\mathbf{d}} = F \sum_{\alpha=1}^{A} z_\alpha \bar{c}_\alpha \quad \text{and} \quad \bar{\mathbf{i}} = F \sum_{\alpha=1}^{A} z_\alpha \bar{\mathbf{j}}_\alpha, \tag{10}$$

and the effective constitutive relations are expressed in terms of effective potentials as

$$\bar{\mathbf{j}}_\alpha = -\bar{c}_\alpha \frac{\partial \widetilde{U}_\alpha}{\partial \bar{\mathbf{g}}}(\nabla \bar{\mu}_\alpha) \quad \text{and} \quad \bar{\mathbf{d}} = \frac{\partial \widetilde{W}_e}{\partial \bar{\mathbf{e}}}(\bar{\mathbf{e}}). \tag{11}$$

Here, the overbar denotes macroscopic fields and the effective potentials are defined as

$$\widetilde{U}_\alpha(\bar{\mathbf{g}}) = \min_{\mathbf{g} \in \mathcal{K}(\bar{\mathbf{g}})} \sum_{r=1}^{N} \theta^{(r)} \left\langle \hat{U}_\alpha^{(r)}(\mathbf{g}) \right\rangle^{(r)} \quad \text{and} \quad \widetilde{W}_e(\bar{\mathbf{e}}) = \min_{\mathbf{e} \in \mathcal{K}(\bar{\mathbf{e}})} \sum_{r=1}^{N} \theta^{(r)} \left\langle \hat{W}_e^{(r)}(\mathbf{e}) \right\rangle^{(r)}, \tag{12}$$

where the local potentials are given by

$$\hat{U}_{\alpha}^{(r)}(\mathbf{g}) = \frac{c_{0\alpha}^{(r)}}{\langle c_{0\alpha}\rangle} U_{\alpha}^{(r)}(\mathbf{g}) \quad \text{and} \quad \hat{W}_{e}^{(r)}(\mathbf{e}) = \frac{\epsilon_0}{2}\mathbf{e}\cdot\mathbf{e} + W_{p}^{(r)^*}(\mathbf{e}). \tag{13}$$

In these expressions, $\langle\cdot\rangle$ and $\langle\cdot\rangle^{(r)}$ denote volume averages over the entire representative volume element of the heterogeneous solid and over the subdomain occupied by phase r, respectively, $\theta^{(r)} = \langle\chi^{(r)}\rangle$ is the volume fraction of phase r, $\mathcal{K}(\bar{\mathbf{a}})$ is the set of gradient vector fields with volume average $\bar{\mathbf{a}}$, and $(\cdot)^*$ denotes a Legendre transformation. The ratio of reference concentrations in expression $(13)_1$ emerges as a consequence of having eliminated the molar concentrations in expression $(9)_3$ for the local fluxes in favor of the electrochemical potentials, which happen to be the primal field variables in the multi-scale analysis. If the local potentials are quadratic functions of their arguments the above expressions reduce to those derived by Curto Sillamoni and Idiart (2015).

Thus, the effective response of the electrolyte is completely determined by the effective potentials (12). Note that these potentials are mathematically decoupled and can therefore be computed independently. This is a consequence of the additive form (7) assumed for the local free energy density. Given our interest in nonlinear ionic transport phenomena we henceforth focus on estimating the dissipation potentials $\widetilde{U}_{\alpha}$. However, it is emphasized that the methodology described below can be used *mutatis mutandis* to estimate the effective potential $\widetilde{W}_e$ as well in view of its similar mathematical structure.

3. Linear-comparison homogenization estimates

Estimates for the effective dissipation potentials are generated here by means of the linear-comparison homogenization method proposed by Ponte Castañeda (2001). This section provides the relevant formulae to compute linear-comparison estimates for composite systems made up of *isotropic* phases. The reader is referred to the article of Ponte Castañeda (2001) for details on the derivation.

3.1. Formulae for material systems with isotropic constituent phases

We consider material systems made up of isotropic constituent phases, so that

$$U_{\alpha}^{(r)}(\mathbf{g}) = u_{\alpha}^{(r)}(|\mathbf{g}|) \quad \text{and} \quad \hat{U}_{\alpha}^{(r)}(\mathbf{g}) = \hat{u}_{\alpha}^{(r)}(|\mathbf{g}|). \tag{14}$$

Given that the effective potentials associated with the various ionic species are mathematically decoupled, we henceforth focus on a single species and ommit the subscript α to ease notation.

The linearized comparison potentials correspond to second-order Taylor-type expansions of the nonlinear potentials of the form

$$\hat{U}_{0}^{(r)}(\mathbf{g}) = \hat{U}^{(r)}(\breve{\mathbf{g}}^{(r)}) + \frac{\partial \hat{U}^{(r)}}{\partial \mathbf{g}}(\breve{\mathbf{g}}^{(r)})\cdot(\mathbf{g}-\breve{\mathbf{g}}^{(r)}) + \frac{1}{2}(\mathbf{g}-\breve{\mathbf{g}}^{(r)})\cdot\mathbf{M}_{0}^{(r)}(\mathbf{g}-\breve{\mathbf{g}}^{(r)}), \tag{15}$$

where the reference gradients $\breve{\mathbf{g}}^{(r)}$ and the linear mobilities $\mathbf{M}_{0}^{(r)}$ are uniform properties in each phase r to be specified. These potentials can be rewritten as

$$\hat{U}_0^{(r)}(\mathbf{g}) = \frac{1}{2}\mathbf{g}\cdot\mathbf{M}_0^{(r)}\mathbf{g} + \mathbf{J}_0^{(r)}\cdot\mathbf{g} + f_0^{(r)}, \tag{16}$$

where

$$\mathbf{J}_0^{(r)} = \frac{\partial \hat{U}^{(r)}}{\partial \mathbf{g}}(\breve{\mathbf{g}}^{(r)}) - \mathbf{M}_0^{(r)}\breve{\mathbf{g}}^{(r)} \quad \text{and} \tag{17}$$

$$f_0^{(r)} = \hat{U}^{(r)}(\breve{\mathbf{g}}^{(r)}) - \frac{\partial \hat{U}^{(r)}}{\partial \mathbf{g}}(\breve{\mathbf{g}}^{(r)})\cdot\breve{\mathbf{g}}^{(r)} + \frac{1}{2}\breve{\mathbf{g}}^{(r)}\cdot\mathbf{M}_0^{(r)}\breve{\mathbf{g}}^{(r)}. \tag{18}$$

The effective potential of the linear-comparison composite is thus

$$\widetilde{U}_0(\overline{\mathbf{g}}) = \min_{\mathbf{g}\in\mathcal{K}(\overline{\mathbf{g}})} \sum_{r=1}^{N} \theta^{(r)} \left\langle \frac{1}{2}\mathbf{g}\cdot\mathbf{M}_0^{(r)}\mathbf{g} + \mathbf{J}_0^{(r)}\cdot\mathbf{g} + f_0^{(r)} \right\rangle^{(r)}. \tag{19}$$

In the case of isotropic phases, the optimal linear-comparison properties $\breve{\mathbf{g}}^{(r)}$ and $\mathbf{M}_0^{(r)}$ are given by

$$\breve{\mathbf{g}}^{(r)} = \overline{\mathbf{g}}^{(r)} \quad \text{and} \quad \mathbf{M}_0^{(r)} = M_{\parallel}^{(r)}\frac{\overline{\mathbf{g}}^{(r)}}{\overline{g}^{(r)}}\otimes\frac{\overline{\mathbf{g}}^{(r)}}{\overline{g}^{(r)}} + M_{\perp}^{(r)}\left[\mathbf{I} - \frac{\overline{\mathbf{g}}^{(r)}}{\overline{g}^{(r)}}\otimes\frac{\overline{\mathbf{g}}^{(r)}}{\overline{g}^{(r)}}\right], \tag{20}$$

where $\overline{\mathbf{g}}^{(r)}$ is the average of $\mathbf{g}(\mathbf{x})$ over phase r in the linear-comparison composite (19), $\overline{g}^{(r)} = |\overline{\mathbf{g}}^{(r)}|$, and the mobilities correspond to generalized-secant linearizations of the nonlinear potentials as given by

$$\hat{u}^{(r)\prime}(\hat{g}^{(r)})\frac{\hat{g}_{\parallel}^{(r)}}{\hat{g}^{(r)}} - \hat{u}^{(r)\prime}(\overline{g}^{(r)}) = M_{\parallel}^{(r)}(\hat{g}_{\parallel}^{(r)} - \overline{g}^{(r)}) \quad \text{and} \quad \frac{\hat{u}^{(r)\prime}(\hat{g}^{(r)})}{\hat{g}^{(r)}} = M_{\perp}^{(r)} \tag{21}$$

with $\hat{g}^{(r)} = \sqrt{(\hat{g}_{\parallel}^{(r)})^2 + (\hat{g}_{\perp}^{(r)})^2}$ and the prime denoting differentiation. In these expressions, the hat variables are related to the first and second moments of the gradient field $\mathbf{g}(\mathbf{x})$ in the linear-comparison composite (19) via

$$\hat{g}_{\parallel}^{(r)} = \overline{g}^{(r)} + \sqrt{C_{\parallel}^{(r)}} \quad \text{and} \quad \hat{g}_{\perp}^{(r)} = \sqrt{C_{\perp}^{(r)}}, \tag{22}$$

where

$$\overline{\mathbf{g}}^{(r)} = \frac{1}{\theta^{(r)}}\frac{\partial(\widetilde{U}_0 - \overline{f}\,)}{\partial \mathbf{J}_0^{(r)}} \quad \text{and} \quad C_{\parallel,\perp}^{(r)} = \frac{2}{\theta^{(r)}}\frac{\partial \widetilde{U}_0}{\partial M_{\parallel,\perp}^{(r)}}. \tag{23}$$

Here, $\overline{f} = \sum_{r=1}^{N}\theta^{(r)}f^{(r)}$, and in the first expression the derivative is taken holding $\mathbf{M}_0^{(r)}$ fixed while in the second expression $\breve{\mathbf{g}}^{(r)}$ is held fixed. The quantities $(23)_2$ correspond to traces of the covariance tensor $\mathbf{C}_{\mathbf{g}}^{(r)} = \langle(\mathbf{g}(\mathbf{x}) - \overline{\mathbf{g}}^{(r)})\otimes(\mathbf{g}(\mathbf{x}) - \overline{\mathbf{g}}^{(r)})\rangle^{(r)}$ within each phase r. Thus, the linearization scheme depends not only on the first moments of the fields but also on the intraphase fluctuations. Given a linear estimate for the effective comparison potential (19), expressions (20) through (23) constitute a system of nonlinear algebraic equations for the quantities $\hat{g}_{\parallel,\perp}^{(r)}$ and $M_{\parallel,\perp}^{(r)}$, $r = 1,...,N$.

Finally, the generalized-secant homogenization estimate for the effective potential is given by

$$\widetilde{U}(\overline{\mathbf{g}}) = \sum_{r=1}^{N} \theta^{(r)} \left[\hat{u}^{(r)}(\hat{g}^{(r)}) - \hat{u}^{(r)\prime}(\overline{g}^{(r)})(\hat{g}_{\|}^{(r)} - \overline{g}^{(r)})\right]. \tag{24}$$

3.2. Formulae for two-phase material systems with power-law dissipation

We now specialize the above formulae to two-phase material systems made up of power-law phases characterized by potentials of the form

$$u^{(r)}(g) = \frac{G_0^{(r)}}{1+m} \left| \frac{g}{G_0^{(r)}} \right|^{1+m}, \tag{25}$$

where the exponent m is the same for all phases. For $m = 1$ this potential corresponds to a linear response with ionic mobility $(G_0^{(r)})^{-1}$, while for $m \to \infty$ it corresponds to a strongly nonlinear response whereby the molar flux is zero if the electrochemical potential gradient has magnitude below the threshold $G_0^{(r)}$ and is unbounded otherwise. Thus, these potentials provide a convenient test case to assess the capabilities of the above linear-comparison method within a wide range of nonlinear responses.

For simplicity, we restrict the analysis to two-phase composites exhibiting overall isotropic symmetry. It then follows that the effective potential must be of the form

$$\widetilde{U}(\overline{\mathbf{g}}) = \frac{\widetilde{G}_0}{1+m} \left| \frac{\overline{\mathbf{g}}}{\widetilde{G}_0} \right|^{1+m}, \tag{26}$$

where m is the same exponent as that of the constituent phases and $\widetilde{G}_0$ is an effective property which depends on the local properties $G_0^{(r)}$, the microstructure, and the exponent m.

Thus, the linear-comparison estimate (24) delivers an estimate for $\widetilde{G}_0$. For the special case of two-phase composites, expression (19) can be greatly simplified by virtue of the so-called Levin relations; it can be written as

$$\widetilde{U}_0(\overline{\mathbf{g}}) = \overline{f}_0 + \overline{J}_0 \cdot \overline{\mathbf{g}} + \frac{1}{2}\overline{\mathbf{g}} \cdot \overline{\mathbf{M}}_0 \overline{\mathbf{g}} + \frac{1}{2}[\overline{\mathbf{g}} + (\Delta \mathbf{M}_0)^{-1}\Delta \mathbf{J}_0] \cdot (\widetilde{\mathbf{M}}_0 - \overline{\mathbf{M}}_0)[\overline{\mathbf{g}} + (\Delta \mathbf{M}_0)^{-1}\Delta \mathbf{J}_0], \tag{27}$$

where $\Delta \mathbf{M}_0 = \mathbf{M}_0^{(2)} - \mathbf{M}_0^{(1)}$ and $\Delta \mathbf{J}_0 = \mathbf{J}_0^{(2)} - \mathbf{J}_0^{(1)}$, and $\widetilde{\mathbf{M}}_0$ is the effective mobility tensor of the linear solid. This linear-comparison potential is thus completely specified in terms of $\widetilde{\mathbf{M}}_0$. So by making use of any linear homogenization estimate for $\widetilde{\mathbf{M}}_0$, corresponding estimates for the nonlinear effective potential can be obtained. In this work we make use of MGA and EMA estimates, which can be generated from the following expression due to Willis (1977):

$$\widetilde{\mathbf{M}}_0 = \left\{ \sum_{r=1}^{2} \theta^{(r)} \mathbf{M}_0^{(r)} [\mathbf{I} + \mathbf{T}^{(0)}(\mathbf{M}_0^{(r)} - \mathbf{M}^{(0)})]^{-1} \right\} \left\{ \sum_{s=1}^{2} \theta^{(s)} [\mathbf{I} + \mathbf{T}^{(0)}(\mathbf{M}_0^{(s)} - \mathbf{M}^{(0)})]^{-1} \right\}^{-1}, \tag{28}$$

where $\mathbf{M}^{(0)}$ denotes the mobility of a homogeneous reference material, and $\mathbf{T}^{(0)}$ is a second-order tensor that depends on $\mathbf{M}^{(0)}$ and the two-point correlation functions of the microstructure. By setting the reference tensor $\mathbf{M}^{(0)}$ equal to $\mathbf{M}_0^{(1)}$ ($\mathbf{M}_0^{(2)}$) we obtain MGA estimates, appropriate for 'particulate' microstructures with phase $r = 1$ ($r = 2$) playing the role of a matrix.

On the other hand, by setting $\mathbf{M}^{(0)}$ equal to the $\widetilde{\mathbf{M}}_0$ we obtain EMA estimates, appropriate for 'granular' microstructures with no continuous matrix phase.

In view of the assumed overall isotropy, the phase averages $\overline{\mathbf{g}}^{(r)}$ are aligned with the overall field $\overline{\mathbf{g}}$. Then, the unit vectors $\overline{\mathbf{g}}^{(r)}/\overline{g}^{(r)} = \overline{\mathbf{g}}/\overline{g}$ are the same for all phases, and the mobility tensors $(20)_2$ in the linear-comparison composite are all aligned. Furthermore, if the tensor $\mathbf{M}^{(0)}$ is of the form $(20)_2$, the tensor $\mathbf{T}^{(0)}$ is also of that form, with 'parallel' and 'perpendicular' components given by (e.g. Ponte Castañeda (2001))

$$T_{\parallel}^{(0)} = k\,\frac{1-\alpha(k)}{(k-1)M_{\parallel}^{(0)}} \quad \text{and} \quad T_{\perp}^{(0)} = \frac{k\,\alpha(k)-1}{2(k-1)M_{\perp}^{(0)}} \quad \text{with} \quad \alpha(k) = \frac{\arcsin\sqrt{(k-1)/k}}{\sqrt{k-1}}, \tag{29}$$

where $k = M_{\parallel}^{(0)}/M_{\perp}^{(0)}$ is the anisotropy ratio of the tensor $\mathbf{M}^{(0)}$. Note that in (29) the anistropy ratio has been assumed to be $k > 1$, but corresponding expressions for $k < 1$ can be obtained by analytic continuation. Expressions (27) through (29) completely specify the effective potential of the linear-comparison composite.

By virtue of (24), the linear-comparison estimate for the effective property $\widetilde{G}_0$ can finally be computed from

$$\widetilde{G}_0^{-m} = \sum_{r=1}^{2} \theta^{(r)} \frac{c_0^{(r)}}{\langle c_0 \rangle} (G_0^{(r)})^{-m} \left\{ \left(\frac{\hat{g}^{(r)}}{\overline{g}} \right)^{m+1} - (m+1) \left(\frac{\overline{g}^{(r)}}{\overline{g}} \right)^{m} \left(\frac{\hat{g}_{\parallel}^{(r)}}{\overline{g}} - \frac{\overline{g}^{(r)}}{\overline{g}} \right) \right\}. \tag{30}$$

where $\langle c_0 \rangle = \theta^{(1)} c_0^{(1)} + \theta^{(2)} c_0^{(2)}$.

3.3. Dual estimates

Constitutive relations (11) can be inverted so that the electrochemical potential gradients are expressed in terms of the molar fluxes via the Legendre duals of the dissipation potentials. The linear-comparison technique of section 3.1 can then be used in a completely analogous fashion to derive estimates for the inverted constitutive relation directly from the dual formulation of the problem. Expressions are omitted for brevity. However, as already noted by Ponte Castañeda (2001), the estimates thus obtained from the primal and dual formulations are *not* in general Legendre duals of each other, i.e. they are not equivalent, as a result of certain approximations made in the optimization of the linear-comparison medium. However, the results provided below show that this so-called *duality gap* is very small and even vanishes in some highly nonlinear cases.

4. Sample results of the MGA type

This section reports sample results for two-phase power-law solids resulting from the use of the Maxwell–Garnett approximation (MGA)—also known as Claussius–Mossotti approximation—to estimate the effective potential of the linear-comparison composite. This approximation is known to be accurate for particulate microstructures with low to moderate concentrations of inclusions (e.g. Milton 2002). Henceforth, the matrix and inclusion phases are identified with $r = 1$ and $r = 2$, respectively. The focus here is on the performance of the above linear-comparison estimates in contexts of strong nonlinearities and heterogeneity

contrasts. We thus restrict the analysis to material systems with uniform reference molar concentrations ($c_0^{(1)} = c_0^{(2)}$) to simplify the description; hence $u^{(r)} = \hat{u}^{(r)}$.

Estimates of the MGA-type follow from setting $\mathbf{M}^{(0)} = \mathbf{M}_0^{(1)}$ in (28). Now, this approximation entails uniform fields within the inclusion phase of the linear-comparison solid; hence

$$\hat{\mathbf{g}}^{(2)} = \overline{\mathbf{g}}^{(2)} \quad \text{and} \tag{31}$$

$$\mathbf{M}_0^{(2)} = \frac{\partial^2 \hat{u}^{(2)}}{\partial \mathbf{g} \partial \mathbf{g}}(\overline{\mathbf{g}}^{(2)}) = \frac{1}{G_0^{(2)}} \left| \frac{\overline{g}^{(2)}}{G_0^{(2)}} \right|^{m-1} \left[m \frac{\overline{\mathbf{g}}}{\overline{g}} \otimes \frac{\overline{\mathbf{g}}}{\overline{g}} + \left(\mathbf{I} - \frac{\overline{\mathbf{g}}}{\overline{g}} \otimes \frac{\overline{\mathbf{g}}}{\overline{g}} \right) \right]. \tag{32}$$

Moreover, for a two-phase system we have that $\overline{\mathbf{g}}^{(2)} = (\overline{\mathbf{g}} - \theta^{(1)} \overline{\mathbf{g}}^{(1)})/\theta^{(2)}$, and so the computation of the linear-comparison estimates can be reduced to a system of three algebraic nonlinear equations for the variables $\hat{g}_{\parallel}^{(1)}$, $\hat{g}_{\perp}^{(1)}$ and $\overline{g}^{(1)}$, which must be solved numerically in general.

The new generalized-secant estimates (GSEC^{+-}) of the MGA type are compared next with the elementary bounds of Weiner^{+-} and the secant estimates (SEC) of the MGA type of Ponte Castañeda (1992). It is recalled that the SEC estimates provide a strict upper bound for the corresponding GSEC estimates. Also included are the full-field numerical simulations by Barrett and Talbot (1996) for composite spheres subject to an affine potential or to a uniform current density on the external boundary. These simulations provide upper and lower bounds (BT^{+-}) for the overall resistivity of a particular class of composites known as composite-sphere assemblages; when the phases are linear, the simulations provide the exact result.

Figures 1(a) and (b) shows various predictions for the effective resistivity $\widetilde{G}_0$, normalized by the resistivity of the matrix phase $G_0^{(1)}$, as a function of the nonlinearity index $m \geqslant 1$, for the choice $\theta^{(1)} = \theta^{(2)} = 0.5$ and two values of the resistivity contrast. We begin by noting that for linear materials the SEC and GSEC estimates agree exactly with the linear MGA estimates on which they are based. These linear estimates are known to be attained by composites with isotropic composite-sphere-assemblage, and that is why the BT results also agree with these estimates in this case. For nonlinear materials, the various methods give somewhat different predictions, but the GSEC estimates are found to satisfy all bounds except the lower bound BT^{-} in the case of resistive inclusions. It is worth noting, however, that the difference is very small and that these BT^{-} bounds demanded heavy numerical calculations which might have introduced some error. As already discussed in section 3.3, the generalized-secant estimates exhibit a duality gap. The dual estimates (GSEC*) are also provided in figures 1(a) and (b) to assess the gap size. The gap is seen to be very small in general and to vanish identically not only in the linear case but also in the limiting case $m \to \infty$. Thus, both formulations provide practically equivalent predictions.

The extremely nonlinear limit $m \to \infty$ corresponds to a composite made up of phases with different thresholds $G_0^{(r)}$ in the electrochemical potential gradient, the composite itself having an effective threshold $\widetilde{G}_0$. In this limit the power-law potentials (25) are no longer strictly convex, the character of the governing equations changes, and discontinuous current density fields become possible. In fact, the results of Donev *et al* (2002) and Duxbury *et al* (2006) show that when the macroscopic field reaches the effective threshold the current flow localizes on a path which is the solution to a 'shortest-path problem'.

For composites with more resistive particles ($G_0^{(2)} > G_0^{(1)}$), the GSEC estimates predict no effect on the effective threshold due to the addition of inclusions, i.e.

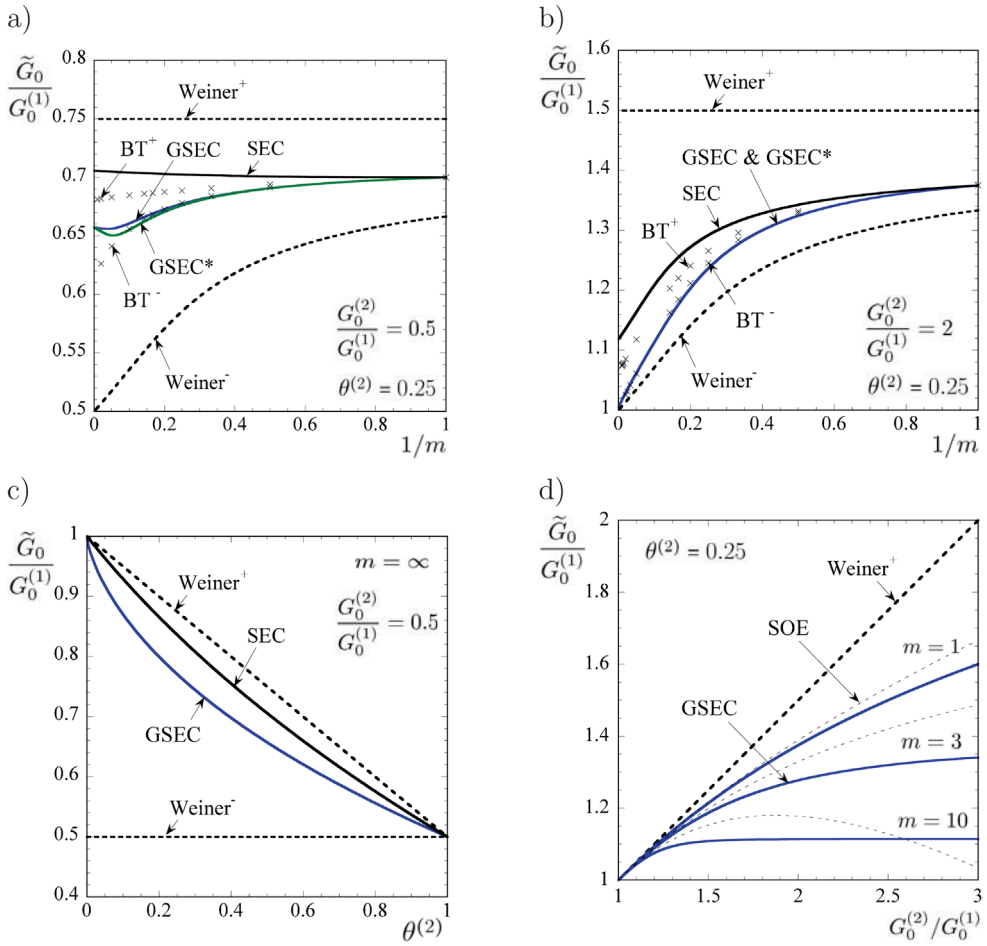

Figure 1. Estimates of the MGA type for the effective resistivity of two-phase composites as a function of material nonlinearity (m), inclusion concentration ($\theta^{(2)}$) and resistivity ratio ($G_0^{(2)}/G_0^{(1)}$).

$$\frac{\widetilde{G}_0}{G_0^{(1)}} = 1 \tag{33}$$

regardless of the particular contrast and concentration of inclusions. According to Donev *et al* (2002), in this case the current path tries to avoid the inclusions but at the same time tries to remain as straight as possible. The GSEC estimates are consistent with totally straight current paths. The SEC and BT^+ bounds, on the other hand, do predict an effect and are therefore consistent with current densities that are either diffuse or localized along curved rather than straight lines. The fact that the BT^+ bound is obtained by prescribing uniform current densities on the boundary of a composite sphere actually prevents it from capturing the presence of localized current fields.

On the other hand, for composites with less resistive inclusions ($G_0^{(2)} < G_0^{(1)}$), the GSEC estimates do predict an effect on the effective threshold due to the addition of inclusions. These estimates can be shown to reduce to

$$\frac{\widetilde{G}_0}{G_0^{(1)}} = \frac{1-\theta^{(2)}}{\sqrt{2\theta^{(2)}}} \frac{1}{k[k\ \alpha(k)-1]} \frac{f_{\parallel}(k)+kf_{\perp}(k)}{\sqrt{f_{\parallel}(k)+f_{\perp}(k)}} + \frac{G_0^{(2)}}{G_0^{(1)}}, \tag{34}$$

where the functions $f_{\parallel}$ and $f_{\perp}$ are given by

$$f_{\parallel}(k) = k\,[1 + k\ \alpha(k)(1-2\alpha(k))] \quad \text{and} \quad f_{\perp}(k) = (2+k)\alpha(k) - 3, \tag{35}$$

and the anisotropy ratio $k > 1$ is solution to the nonlinear equation

$$1-\alpha(k) = \sqrt{\frac{\theta^{(2)}}{2}}\left(\frac{k-1}{k}\sqrt{f_{\parallel}(k)} - \frac{G_0^{(2)}}{G_0^{(1)}}\sqrt{f_{\parallel}(k)+f_{\perp}(k)}\right). \tag{36}$$

According to Duxbury *et al* (2006), in this case the current path seeks the inclusions but at the same time tries to remain as straight as possible. Consequently, the inclusions interact even when their volume fraction is infinitesimally small. This is expected to translate into a non-analytic dilute expansion of the effective threshold. Interestingly, this is exactly what the GSEC estimates predict. Figure 1(c) shows GSEC estimates for $G_0^{(2)}/G_0^{(1)} = 0.5$ as a function of inclusion concentration $\theta^{(2)}$, together with the corresponding SEC and Weiner bounds. Indeed, it is observed that, while the bounds exhibit a finite slope at $\theta^{(2)} = 0$, the GSEC estimates exhibit an infinite slope. It can be shown that the dilute expansion of (34) is

$$\frac{\widetilde{G}_0}{G_0^{(1)}} = 1 - \frac{3}{2}\left(1 - \frac{G_0^{(2)}}{G_0^{(1)}}\right)^{4/3}\left(\frac{\pi}{2}\right)^{2/3}\left(\frac{\theta^{(2)}}{2}\right)^{2/3}, \tag{37}$$

which is non-analytic at $\theta^{(2)} = 0$. This 'dilute-limit singularity' has also been observed in the dielectric breakdown of discrete (Duxbury *et al* 1995) and continuum (Duxbury *et al* 1990) heterogeneous media, as well as in ductile fracture of porous media (Roux and François 1991). A similar dilute expansion with a 2/3 exponent has been found in two-dimensional random composite dielectrics (Ponte Castañeda 2001). Different singularities appear, however, in periodic composites. Consider a cubic array of spherical inclusions embedded in a matrix with a higher threshold. In that case the shortest path corresponds to a straight line passing through the inclusions. It is straightforward to see that these fields imply that $1 - \widetilde{G}_0/G_0^{(1)} \sim (\theta^{(2)})^{1/3}$—see Idiart *et al* (2009) for a similar analysis in two-dimensional viscoplastic solids. A comparison with expression (37) suggests that randomness weakens the dilute-limit singularity. In any event, it is a remarkable fact that the generalized-secant estimates are able to capture such strongly nonlinear effects. We note in passing that particle-filled composites often exhibit non-monotonic variations of resistivity with filler volume fraction, and that such variations can usually be ascribed to the presence of interphases surrounding the particles. While accounting for interphases in the context of stochastics models like the one considered here has proven challenging, they can be accounted for in the context of solvable microgeometries as in, for instance, Curto Sillamoni and Idiart (2015).

Finally, in figure 1(d) the GSEC estimates are plotted as a function of the heterogeneity contrast, with $G_0^{(2)} \geqslant G_0^{(1)}$, for several values of the nonlinearity index ($m = 1, 3, 10, \infty$). These estimates are compared with the Weiner upper bound, which is insensitive to m, and the exact second-order asymptotic expansion (SOE) of Blumenfeld and Bergman (1991). It should be noted that the range of validity of this expansion vanishes as $m \to \infty$, whereas the GSEC estimates, which are also exact to second order in the contrast, do not degenerate. It is observed that as the nonlinearity increases the GSEC estimates tend to saturate at smaller contrasts. Thus, nonlinearity amplifies the effect of heterogeneity contrast.

5. Sample results of the EMA type

This section reports sample results for two-phase power-law solids resulting from the use of the effective-medium approximation (EMA) of Bruggeman (1935) to estimate the effective potential of the linear-comparison composite. This approximation is more appropriate for granular microstructures (e.g. Milton 2002). Estimates of the EMA-type are obtained by setting $\mathbf{M}^{(0)} = \widetilde{\mathbf{M}}_0$ in expression (28). Unlike the MGA approximation, this approximation does not entail uniform fields in any of the phases. Furthermore, expression (28) is no longer explicit for $\widetilde{\mathbf{M}}_0$, thus rendering two nonlinear equations for the effective mobilities $\widetilde{M}_{\parallel,\perp}$, in addition to the five equations for the variables $\hat{g}^{(r)}_{\parallel,\perp}$ and $\overline{g}^{(1)}$. This system of nonlinear equations must be solved numerically.

The new generalized-secant estimates (GSEC) of the EMA type are compared next with the elementary bounds of Weiner and the secant estimates (SEC) of the EMA type of Ponte Castañeda (1992). Recall that the SEC estimates provide strict upper bound for the corresponding GSEC estimates. Figures 2(a) and (b) shows various predictions for the effective resistivity $\widetilde{G}_0$, normalized by the resistivity $G_0^{(1)}$, as a function of the nonlinearity index $m \geqslant 1$, for $\theta^{(2)} = 0.25$ and the two extreme values of resistivity contrast. In the linear case, the SEC and GSEC estimates agree exactly with the linear EMA estimates on which they are based. In the nonlinear case, however, these estimates give different predictions with the GSEC estimates always lying below the SEC estimates as they should. A comparison with the previous results of figure 1 shows that, unlike the elementary bounds of Weiner, the linear-comparison estimates are able to capture a certain interplay between the microstructure and the material nonlinearity. The dual generalized-secant estimates (GSEC$*$) are also included to assess the magnitude of the duality gap. Once again, the gap is found to be very small in general but to vanish identically as $m \to \infty$ only when $G_0^{(2)} = 0$. When $G_0^{(2)} = \infty$ a duality gap persists in the limit $m \to \infty$, even though it is so small that both estimates can be considered virtually equivalent also in this case.

Unlike the GSEC estimates of the MGA type, the GSEC estimates of the EMA type for $m \to \infty$ predict a finite effect on the effective threshold due to the addition of a second phase regardless of the contrast in the local thresholds. In this extremely nonlinear limit, the GSEC estimates for material systems with phase $r = 2$ being a perfect ionic conductor ($G_0^{(2)} = 0$) can be shown to reduce to

$$\frac{\widetilde{G}_0}{G_0^{(1)}} = (1-\theta^{(2)})\left[\left(1+\sqrt{\frac{\theta^{(2)}}{2}\frac{g_{\parallel}(\tilde{k})}{g(\tilde{k})}}\right)^2 + \frac{\theta^{(2)}}{2}\frac{g_{\perp}(\tilde{k})}{g(\tilde{k})}\right]^{-1/2}, \tag{38}$$

where the functions g are too cumbersome to include here and are given in the appendix; these are functions of the effective anisotropy ratio $\tilde{k} = \widetilde{M}_{\parallel}/\widetilde{M}_{\perp}$, which solves the nonlinear equation

$$\frac{\theta^{(2)}}{2}\frac{g_{\parallel}(\tilde{k})}{g(\tilde{k})} = \frac{1}{(k-1)^2} \tag{39}$$

with the anisotropy ratio k of phase $r = 1$ given by

$$k = \frac{1-\tilde{k}\ \alpha(\tilde{k})}{1-\alpha(\tilde{k})}\ \frac{\theta^{(2)}+\tilde{k}(1-\theta^{(2)})-\tilde{k}\ \alpha(\tilde{k})}{1-2\,\theta^{(2)}\,(1-\tilde{k})-\tilde{k}\ \alpha(\tilde{k})}. \tag{40}$$

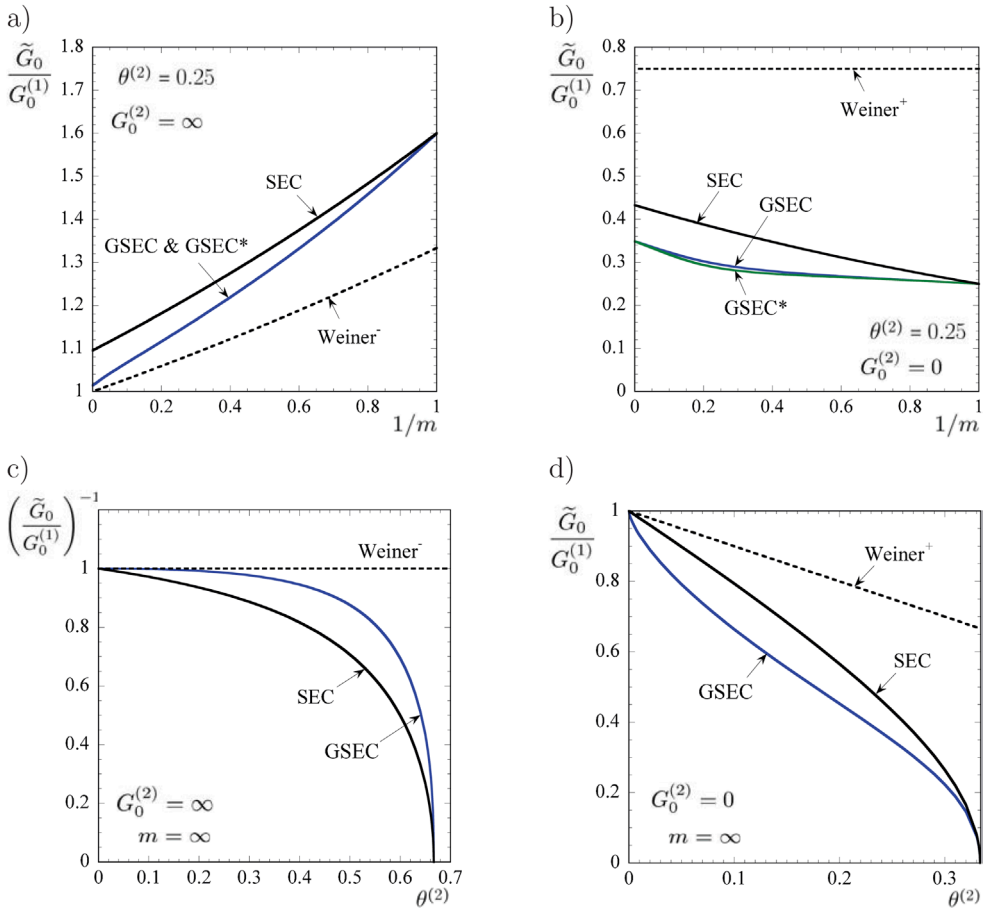

Figure 2. Estimates of the EMA type for the effective resistivity of two-phase composites as a function of material nonlinearity (m) and inclusion concentration ($\theta^{(2)}$).

On the other hand, the GSEC*[3] estimates for material systems with phase $r = 2$ being a perfect ionic insulator ($G_0^{(2)} = \infty$) can be shown to reduce to

$$\frac{\widetilde{G}_0}{G_0^{(1)}} = \left[\left(1 + \sqrt{\theta^{(2)}\frac{h_{\parallel}(\widetilde{k})}{h(\widetilde{k})}}\right)^2 + \theta^{(2)}\frac{h_{\perp}(\widetilde{k})}{h(\widetilde{k})}\right]^{1/2} - \sqrt{\theta^{(2)}\frac{h_{\parallel}(\widetilde{k})}{h(\widetilde{k})}}, \tag{41}$$

where the functions h are given in the appendix; these are functions of the effective anisotropy ratio $\widetilde{k}$, which solves the nonlinear equation

$$\left(1 + \sqrt{\theta^{(2)}\frac{h_{\parallel}(\widetilde{k})}{h(\widetilde{k})}}\right)^2 + \theta^{(2)}\frac{h_{\perp}(\widetilde{k})}{h(\widetilde{k})} = \left(1 + \frac{k-1}{k}\sqrt{\theta^{(2)}\frac{h_{\parallel}(\widetilde{k})}{h(\widetilde{k})}}\right)^2 \tag{42}$$

with the anisotropy ratio k of phase $r = 1$ given by

[3] In this case the mathematical expressions obtained with the dual formulation are much simpler than those obtained with the primal formulation.

$$k = (\tilde{k}\ \alpha(\tilde{k}) - 1)\ \tilde{k}\ \frac{1 + \tilde{k}\ (\alpha(\tilde{k}) - 2) + 2\ \theta^{(2)}\ (\tilde{k} - 1)}{[(\tilde{k}\ \alpha(\tilde{k}) - 1) - \theta^{(2)}\ (\tilde{k} - 1)]\ [1 + (\alpha(\tilde{k}) - 2)\tilde{k}]}. \tag{43}$$

The estimates are plotted in figures 2(c) and (d) versus volume fraction $\theta^{(2)}$. In the dilute limit $\theta^{(2)} \to 0$ these estimates agree exactly to 'first' order with the dilute expansions of the corresponding estimates of the MGA type. This is because the EMA and MGA linear estimates on which they are based exhibit the same dilute behavior. Thus, GSEC estimates of the EMA type also exhibit dilute singularities and are consistent with localized fields as discussed in the context of the MGA estimates. For large concentrations $\theta^{(2)}$, however, the GSEC estimates of the EMA type exhibit percolative behavior near a critical volume fraction $\theta_c^{(2)} < 1$. This percolation threshold is the same as that of the linear EMA theory on which the GSEC estimates are based, thus depending on the spatial dimensionality of the fields but not on the material nonlinearity, as it should. In the case of phase $r = 2$ being a perfect insulator ($G_0^{(2)} = \infty$) percolation occurs at the critical value $\theta_c^{(2)} = 2/3$, while in the opposite case of phase $r = 2$ being a perfect conductor ($G_0^{(2)} = 0$) percolation occurs at the lower critical value $\theta_c^{(2)} = 1/3$. Near these percolation thresholds the effective nonlinear resistivity behaves like $\widetilde{G}_0 \sim G_0^{(1)}(\theta_c^{(2)} - \theta^{(2)})^{\pm s}$, where s is a critical exponent. Given the bounding property of the SEC estimates, which also percolate, this exponent must satisfy the lower bound $s \geqslant 1/2$ for $G_0^{(2)} = \infty$ and the upper bound $s \leqslant 1/2$ for $G_0^{(2)} = 0$. By expanding expressions (38) and (41), it can be verified that the GSEC estimates exhibit percolative behavior with exponents $s = \pm\, 1/2$, which are identical to those bounds. In this connection, it is worth noting that an earlier linear-comparison technique proposed by Ponte Castañeda and Kailasam (1997) and based on a tangent linearization about the phase averages yielded critical exponents of $s = 0$ for $G_0^{(2)} = \infty$ and $s = 1$ for $G_0^{(2)} = 0$, thus violating the bounds. As already noted by Ponte Castañeda (2001), this improvement of the generalized-secant estimates relative to the tangent estimates is directly linked to the use of the field fluctuations—which become unbounded at percolation—in the linearization scheme.

We conclude this discussion by noting that the linear-comparison solid underlying the GSEC estimates of the EMA type can exhibit negative-definite mobility tensors when the nonlinearity is sufficiently high. Indeed, even though $\tilde{k} > 0$ for any value of m, the associated anisotropy ratio k becomes negative for sufficiently large values of m. In rigour, the corresponding effective potential $\widetilde{U}_0$, as given by (19), is no longer a minimum but a stationary value. This raises some questions about the validity of these EMA estimates for power-law composites with sufficiently high nonlinearities, even though the issue is not exclusively due to the use of the linear EMA estimates—Idiart and Ponte Castañeda (2005) already identified this issue in generalized-secant estimates for viscoplastic composites resulting from the use of a different linear scheme. Nevertheless, the estimates for the effective nonlinear resistivity still satisfy rigorous bounds and give reasonable predictions. In the course of this work, Ponte Castañeda (2015) proposed a reformulation of the generalized-secant technique which could deliver more accuracte predictions and be free of this mathematical deficiency. While this reformulation is thus far available for crystalline solids only, it can be adapted to other types of solids including those considered here. Further efforts should be directed towards this goal.

Acknowledgments

This work was funded by the Agencia Nacional de Promoción Científica y Tecnológica through grants PRH-2007-15 and PICT-2014-198, and by CONICET through a doctoral fellowship for

I.J.C.S. Additional support from the Universidad Nacional de La Plata through grant I-2013-179 is also gratefully acknowledged.

Appendix. Expressions for nonlinear estimates of the EMA type

The g functions appearing in expressions (38) and (39) are given by

$$\begin{aligned} g_{\parallel}(\tilde{k}) = &-(1-2\,\theta^{(2)}+8\,\theta^{(2)}\,\tilde{k})+(1+10\,\theta^{(2)}+8\,\theta^{(2)}\,\tilde{k})\tilde{k}\;\alpha(\tilde{k}) \\ &+(2-8\,\theta^{(2)}+(1-10\,\theta^{(2)})\,\tilde{k})\,\tilde{k}\;\alpha(\tilde{k})^2 \\ &-(4-8\,\theta^{(2)}+(1+2\,\theta^{(2)})\,\tilde{k})\,\tilde{k}^2\,\alpha(\tilde{k})^3+2\,\tilde{k}^3\,\alpha(\tilde{k})^4, \end{aligned} \tag{A.1}$$

$$g_{\perp}(\tilde{k}) = (1-\theta^{(2)})\,\tilde{k}\;(\tilde{k}\;\alpha(\tilde{k})-1)^2\,(3-(2+\tilde{k})\,\alpha(\tilde{k})), \tag{A.2}$$

$$\begin{aligned} g(\tilde{k}) = &\frac{\theta^{(2)}}{2}(1-2\,\theta^{(2)})-(1-3\,\theta^{(2)}-2\,(\theta^{(2)})^2)\,\tilde{k}+(1-\theta^{(2)})\theta^{(2)}\,\tilde{k}^2 \\ &+\left[\left(2-\frac{13}{2}\,\theta^{(2)}-(\theta^{(2)})^2\right)\tilde{k}+2\,(1-4\,\theta^{(2)}+(\theta^{(2)})^2)\,\tilde{k}^2+\theta^{(2)}(1-\theta^{(2)})\,\tilde{k}^3\right]\alpha(\tilde{k}) \\ &-\left[(1-2\,\theta^{(2)}-2\,(\theta^{(2)})^2)+\left(4-\frac{25}{2}\,\theta^{(2)}+4\,(\theta^{(2)})^2\right)\tilde{k}+(1+\theta^{(2)}-2\,(\theta^{(2)})^2)\,\tilde{k}^2\right]\tilde{k}\;\alpha(\tilde{k})^2 \\ &+\left[2\,(1-2\,\theta^{(2)})+\left(2-\frac{\theta^{(2)}}{2}\right)\tilde{k}\right]\tilde{k}^2\,\alpha(\tilde{k})^3-\tilde{k}^3\,\alpha(\tilde{k})^4. \end{aligned} \tag{A.3}$$

The h functions appearing in expressions (41) and (42) are given by

$$\begin{aligned} h_{\parallel}(\tilde{k}) = &[(1+\tilde{k}\;(\alpha(\tilde{k})-2))^2\,(\tilde{k}\;\alpha(\tilde{k})\,(2\,\alpha(\tilde{k})-1)-1) \\ &+2\,\theta^{(2)}\,(1-\tilde{k}\;(6-7\,\alpha(\tilde{k})+4\,\alpha(\tilde{k})^2)+\tilde{k}^2\,(2+\alpha(\tilde{k})^2) \\ &+\tilde{k}^3\,\alpha(\tilde{k})\,(2-6\,\alpha(\tilde{k})+3\,\alpha(\tilde{k})^2))]\,\tilde{k}, \end{aligned} \tag{A.4}$$

$$h_{\perp}(\tilde{k}) = (1-\theta^{(2)})[1-\tilde{k}\;(2-\alpha(\tilde{k}))]^2\;\;[3-(2+\tilde{k})\,\alpha(\tilde{k})]\,, \tag{A.5}$$

$$\begin{aligned} h(\tilde{k}) = &-2(-1+2\,\tilde{k}+(\alpha(\tilde{k})-2)\,\alpha(\tilde{k})\,\tilde{k}^2)^2 \\ &+4\,(\theta^{(2)})^2\,(\tilde{k}-1)^2\,(-1+(\alpha(\tilde{k})-1)\tilde{k}^2\,\alpha(\tilde{k}) \\ &+\tilde{k}\;(2\,\alpha(\tilde{k})-1))+\theta^{(2)}\,(6-\tilde{k}\;(13+8\,\alpha(\tilde{k})) \\ &+\tilde{k}^4\,\alpha(\tilde{k})\,(4+4\,\alpha(\tilde{k})-5\,\alpha(\tilde{k})^2)+\tilde{k}^2\,(12+17\,\alpha(\tilde{k}) \\ &-2\,\alpha(\tilde{k})^2)+\tilde{k}^3\,(4-40\,\alpha(\tilde{k})+25\,\alpha(\tilde{k})^2-4\,\alpha(\tilde{k})^3)). \end{aligned} \tag{A.6}$$

References

Allaire G and Briane M 1996 Multiscale convergence and reiterated homogenization *Proc. R. Soc. Edinburgh* **126A** 297–342

Barrett K E and Talbot D R S 1996 Bounds for the effective properties of a nonlinear two-phase composite dielectric *Proc. 8th Int. Symp. Continuum Models and Discrete Systems* ed K Z Markov (Singapore: World Scientific) pp 92–9

Blumenfeld R and Bergman D J 1991 Strongly nonlinear composite dielectrics: a perturbation method for finding the potential field and bulk effective properties *Phys. Rev.* B **44** 7378–86
Bruggeman D A G 1935 *Ann. Phys., Lpz.* **24** 636
Curto Sillamoni I and Idiart I 2015 A model problem concerning ionic transport in microstructured solid electrolytes *Contin. Mech. Thermodyn.* **27** 941–57
Donev A, Musolff C E and Duxbury P M 2002 Random manifolds in non-linear resistor networks: applications to varistors and superconductors *J. Phys. A: Math. Gen.* **35** L327
Duxbury P M, Beale P D, Bak H and Shroeder P A 1990 *J. Phys. D: Appl. Phys.* **23** 1546
Duxbury P M Beale P D and Moukarzel C 1995 *Phys. Rev.* B **51** 3476
Duxbury P M, McGarrity E S and Holm E A 2006 Critical manifolds in non-linear response of complex materials *Mech. Mater.* **38** 757–71
Heuer A, Murugavel S and Roling B 2005 Nonlinear ionic conductivity of thin solid electrolyte samples: comparison between theory and experiment *Phys. Rev.* B **72** 174304
Hong W, Zhao X and Suo Z 2010 Large deformation and electrochemistry of polyelectrolyte gels *J. Mech. Phys. Solids* **58** 558–77
Idiart M I and Ponte Castañeda P 2005 Second-order estimates for nonlinear isotropic composites with spherical pores and rigid particles *C. R. Mec.* **333** 147–54
Idiart M I, Willot F, Pellegrini Y-P and Ponte Castañeda P 2009 Infinite-contrast periodic composites with strongly nonlinear behavior: effective-medium theory versus full-field simulations *Int. J. Solids Struct.* **46** 3365–82
Milton G W 2002 *The Theory of Composites* (Cambridge: Cambridge University Press)
Ponte Castañeda P 1992 Bounds and estimates for the properties of nonlinear heterogeneous systems *Phil. Trans. R. Soc. Lond.* A **340** 531–67.
Ponte Castañeda P 2001 Second-order theory for nonlinear dielectric composites incorporating field fluctuations *Phys. Rev.* B **64** 214205
Ponte Castañeda P 2015 Fully optimized second-order variational estimates for the macroscopic response and field statistics in viscoplastic crystalline composites *Proc. R. Soc.* A **471** 20150665
Ponte Castañeda P and Kailasam M 1997 Nonlinear electrical conductivity in heterogeneous media *Proc. R. Soc. Lond.* A **453** 793–816
Roux S and François D 1991 A simple model for ductile fracture of porous materials *Scr. Met.* **25** 1087–92
Xiao Y and Bhattacharya K 2008 A continuum theory of deformable, semiconducting ferroelectrics *Arch. Ration. Mech. Anal.* **189** 59–95
Willis J R 1977 Bounds and self-consistent estimates for the overall moduli of anisotropic composites *J. Mech. Phys. Solids* **25** 185–202